Structural Engineering and Mechanics, Vol. 26, No. 2 (2007) 111-126 111
DOI: http://dx.doi.org/10.12989/sem.2007.26.2.111

Seismic response of a monorail bridge incorporating train-bridge interaction

Chul-Woo Kim† and Mitsuo Kawatani‡

Department of Civil Engineering, Kobe University, 1-1 Rokkodai, Nada, Kobe 657-8501, Japan

Chang-Hun Lee‡† and Nobuo Nishimura‡‡

Department of Civil Engineering, Osaka University, Osaka 565-0871, Japan

(Received March 21, 2005, Accepted November 14, 2006)

Abstract. Dynamic responses of the bridge for a straddle-type monorail subjected to the ground motion of high probability to occur are investigated by means of a three-dimensional traffic-induced vibration analysis to clarify the effect of a train's dynamic system on seismic responses of a monorail bridge. A 15DOFs model is assumed for a car in the monorail train. The validity of developed equations of motion for a monorail train-bridge interaction system is verified by comparison with the field-test data. The inertia effect due to a ground motion is combined with the monorail train-bridge interaction system to investigate the seismic response of the monorail bridge under a moving train. An interesting result is that the dynamic system of the train on monorail bridges can act as a damper during earthquakes. The observation of numerical results also points out that the damper effect due to the dynamic system of the monorail train tends to decrease with increasing speed of the train.

Keywords: seismic response; damper effect; monorail train-bridge interaction; straddle-type monorail.

1. Introduction

Good seismic performance of bridge and building structures is an issue of great concern in the countries located in earthquake-prone regions. The design of civil infrastructures considering a life-cycle cost has also been another important consideration. To satisfy both safety and economy in seismic design, it needs better understanding about the mechanism of structural systems in ground motion.

After Northridge and Kobe earthquakes those attacked modernized major cities of USA and Japan, it has been recognized that there is a high possibility to encounter an earthquake during rush hour. The effect of the live load on seismic resistance is generally not taken into account in the highway bridge design code of Japan, while the live load effects are considered in the design of

† COE Research Associate, Corresponding author, E-mail: cwkim@kobe-u.ac.jp
‡ Professor
‡†Ph.D. Candidate
‡‡ Professor

railway bridges including the bridge for new transportations such as monorail system because of a large portion of the train's weight compared with the dead load of the bridge. However, it is obviously not realistic to treat the train on the bridge just as additional mass in seismic design, since the train has a complicate dynamic system.

Rather limited efforts have been devoted to the effect of train dynamics on the seismic resistance of bridges in spite of some interesting studies for dynamic stability of trains or vehicles under a ground motion. Kameda *et al.* (1999) investigated the effect of vehicle loadings on the seismic response of highway bridges. They concluded that the seismic response of the bridge can increase/decrease according to the phase difference between the vehicle and bridge systems. Maruyama and Yamazaki (2002) studied the dynamic response of a vehicle under earthquakes without considering the interaction with bridge structures. Miyamoto *et al*. (1997) investigated the running safety of trains under an earthquake, and the train is set to be stationary on the track. Yang and Wu (2002) studied the dynamic stability of trains moving over bridges shaken by earthquakes.

As for monorail system, it has recently been adopted as one of new transportation systems to solve traffic problems in major cities of the world, including Japan such as Tokyo, Osaka, etc. An interesting feature of the monorail system in Japan is in the straddle-type monorail: the bogie system comprises steering and stabilizing wheels that firmly grasp the track girder (see Fig. 1) to increase running stability. The adoption of the straddle-type system allows the monorail train to act as a sprung mass on the track-girder under earthquakes. Moreover, the weight of a monorail train reaches up to 50% of the bridge weight. No investigation, however, has addressed the effect of the train's dynamic system on seismic performance of the monorail bridge.

In this study, the seismic response of a monorail bridge incorporating train-bridge interaction is examined using a three-dimensional analysis procedure. The validity of equations of motion for a monorail train-bridge interaction system is verified by comparing with the field-test data of traffic-induced vibration of a steel monorail bridge. The Level 1 ground motion of JSHB (Japanese Specifications for Highway Bridges) (Japan Road Association 2002) is used as the earthquake with high probability to occur. It is assumed that both important and standard bridges should behave in an elastic manner without essential damage under the Level 1 ground motion according to the code (Japan Road Association 2002).

The seismic performance level specified in JSHB under the Level 1 ground motion consists of a falling-down prevention of bridges for safety. The shear capacity of bearings, therefore, is

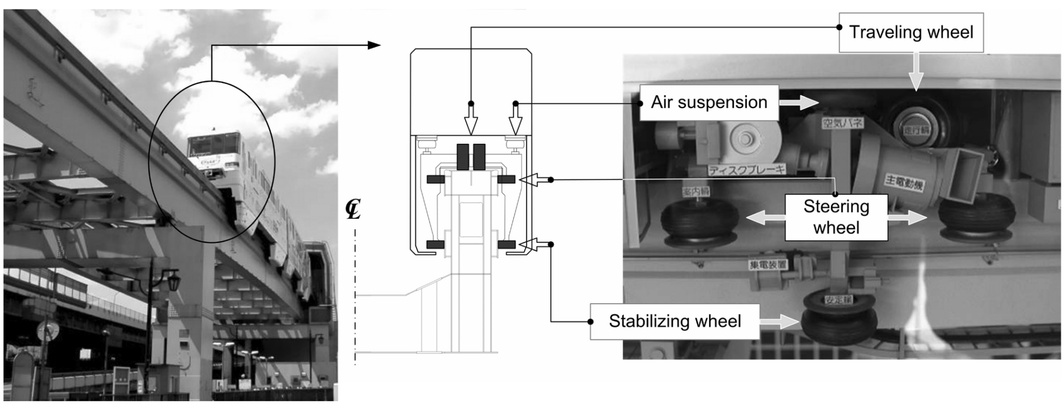

Fig. 1 Configuration of straddle-type monorail train on track girder

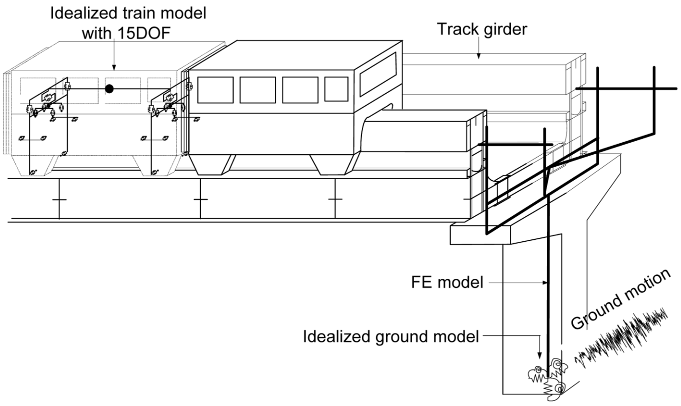

Fig. 2 Scheme for monorail train-bridge interaction system under earthquake

investigated. Investigations are also focused on the acceleration response at the span center of a monorail bridge to determine the effect of the train's dynamic system on dynamic serviceability of the monorail bridge.

2. Monorail train-bridge interaction incorporating with ground motion

The dynamic equilibrium equation of motion for a monorail train-bridge interaction system subjected to earthquakes is developed considering the seismic load as an additional load of the interaction system. Fig. 2 presents the scheme of the monorail train-bridge system subjected to an earthquake.

The monorail train-bridge interaction that satisfies a compatibility condition at the contact point of a tire and bridge is a kind of non-stationary dynamic system when the train starts to move. In order to derive equations of motion for the interactive system, firstly, the monorail train and bridge are modeled separately, and then are combined by using the interaction force/wheel load at the contact point. The authors other work (Lee *et al.* 2006) provides more details in derivation of equations of motion for the monorail train-bridge interactive system. This study assumes that each tire contacts with the track girder during operation even under moderate earthquakes. It is based on the finite element method for modal analysis of the bridge model. The Guyan (1965) reduction is performed to improve the calculation efficiency, even though six-degree-of-freedom is assigned to each node of the bridge model.

2.1 Train model

Fig. 3 shows the numerical model of a monorail train. Equations of motion for the train are obtainable from Lagrange's formulation as follows

$$\frac{\partial}{\partial t}\left(\frac{\partial T}{\partial \dot{a}_i}\right) - \frac{\partial T}{\partial a_i} + \frac{\partial U_e}{\partial a_i} + \frac{\partial U_d}{\partial \dot{a}_i} = 0 \tag{1}$$

where, T is the kinetic energy, U_e is the potential energy of the system and U_d is the dissipation energy due to damping of the system, a_i is a generalized coordinates.

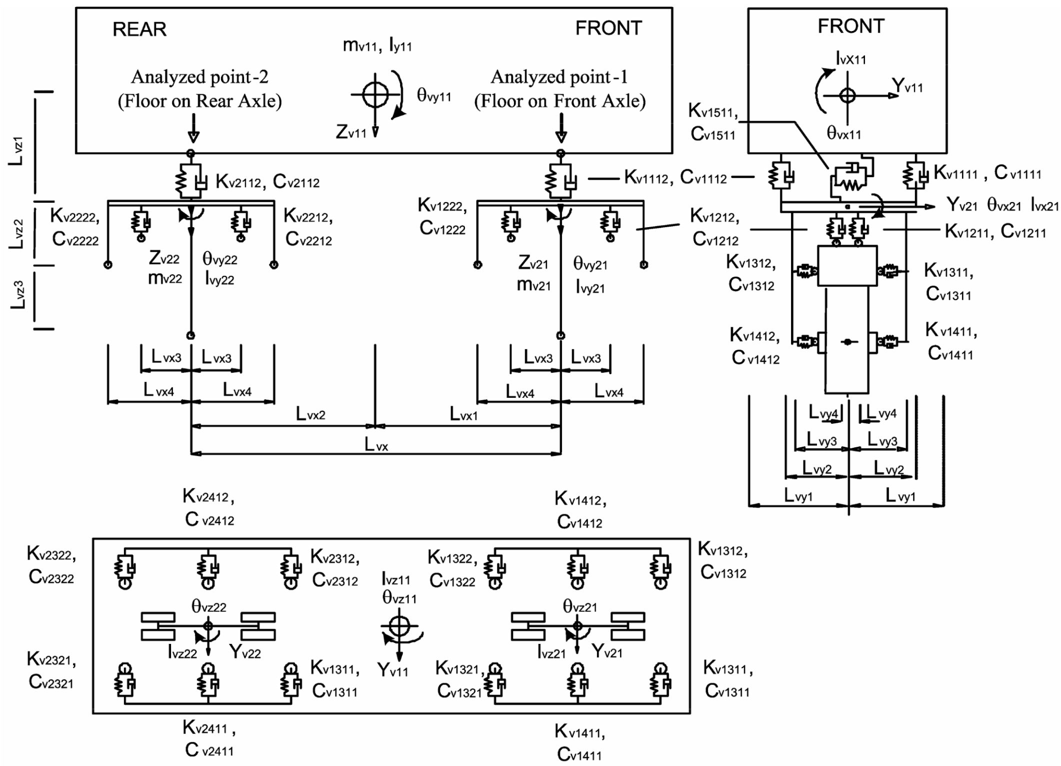

Fig. 3 Numerical monorail train model with 15DOFs

The kinetic energy, potential energy and dissipation energy of the monorail train on a monorail bridge are developed by modifying the energy equation for a vehicle on a highway bridge (Kawatani and Kim 2001). These are expressed in a set of generalized coordinates as follows

$$T = \frac{1}{2}\sum_{v=1}^{nv}[m_{v11}\dot{Z}_{v11}^{2} + m_{v11}\dot{Y}_{v11}^{2} + I_{vx11}\dot{\theta}_{vx11}^{2} + I_{vy11}\dot{\theta}_{vy11}^{2} + I_{vz11}\dot{\theta}_{vz11}^{2}$$
$$+ \sum_{i=1}^{2}\{m_{v2i}\dot{Z}_{v2i}^{2} + m_{v2i}\dot{Y}_{v2i}^{2} + I_{vx2i}\dot{\theta}_{vx2i}^{2} + I_{vy2i}\dot{\theta}_{vy2i}^{2} + I_{vz2i}\dot{\theta}_{vz2i}^{2}\}] \quad (2)$$

$$U_e = \frac{1}{2}\sum_{v=1}^{nv}\left[\sum_{i=1}^{2}\sum_{j=1}^{2}\sum_{n=1}^{2}\{K_{vi1jn}R_{vi1jn}^{2}\delta_{1j} + K_{vi2jn}R_{vi2jn}^{2} + K_{vi3jn}R_{vi3jn}^{2} + K_{vi4jn}R_{vi4jn}^{2}\delta_{1j}\}\right.$$
$$\left. + \sum_{i=1}^{2}K_{vi511}R_{vi511}^{2}\right] \quad (3)$$

$$U_d = \frac{1}{2}\sum_{v=1}^{nv}\left[\sum_{i=1}^{2}\sum_{j=1}^{2}\sum_{n=1}^{2}\{C_{vi1jn}\dot{R}_{vi1jn}^{2}\delta_{1j} + C_{vi2jn}\dot{R}_{vi2jn}^{2} + C_{vi3jn}\dot{R}_{vi3jn}^{2} + C_{vi4jn}\dot{R}_{vi4jn}^{2}\delta_{1j}\}\right.$$
$$\left. + \sum_{i=1}^{2}C_{vi511}\dot{R}_{vi511}^{2}\right] \quad (4)$$

Table 1 Parameters and dynamic characteristics of monorail train (no passenger)

Parameter		Notation	Value
Mass (ton)	Body	m_{v11}	14.22
	Bogie	m_{v21} (=m_{v22})	6.20
Spring constant (kN/m)	Air suspension (vertical)	K_{v1111} (=K_{v1112}=K_{v2111}=K_{v2112})	900.0
	Traveling wheels	K_{v1211} (=K_{v1212}=K_{v1221}=K_{v1222}=K_{v2211}=K_{v2212}=K_{v2221}=K_{v2222})	5170.0
	Steering wheels	K_{v1311} (=K_{v1312}=K_{v1321}=K_{v1322}=K_{v2311}=K_{v2312}=K_{v2321}=K_{v2322})	6370.0
	Stabilizing wheels	K_{v1411} (=K_{v1412}=K_{v2411}=K_{v2412})	6370.0
	Air suspension (lateral)	K_{v1511} (=K_{v2511})	980.0
Damping coefficient (kN·s/m)	Air suspension (vertical)	C_{v1111} (=C_{v1112}=C_{v2111}=C_{v2112})	22.8
	Traveling wheels	C_{v1211} (=C_{v1212}=C_{v1221}=C_{v1222}=C_{v2211}=C_{v2212}=C_{v2221}=C_{v2222})	26.1
	Steering wheels	C_{v1311} (=C_{v1312}=C_{v1321}=C_{v1322}=C_{v2311}=C_{v2312}=C_{v2321}=C_{v2322})	185.5
	Stabilizing wheels	C_{v1411} (=C_{v1412}=C_{v2411}=C_{v2412})	185.5
	Air suspension (lateral)	C_{v1511} (=C_{v2511})	333.6
Geometry (m)		λ_{x1} (=λ_{x2})	4.80
		λ_{x3}	0.75
		λ_{x4}	1.25
		λ_{y1}	1.490
		λ_{y2}	1.025
		λ_{y3}	0.782
		λ_{y4}	0.2
		λ_{z1}	0.885
		λ_{z2}	0.630
		λ_{z3}	1.715

In Eqs. (2), (3) and (4), nv is the number of monorail trains, I is the mass moment of inertia, R_{vimjn} is the relative displacement at springs/dampers, and δ_{ij} is Kronecker's delta. The subscript v is the number of trains on the bridge, the subscript i is an index indicating the suspension position of a train (i = 1 and 2 are the front and rear suspensions, respectively), the subscript j is the tire position in a bogie (e.g., j = 1 and 2 are the front and rear tires of the bogie system, respectively), and n is an index indicating the left and right sides of a train.

Table 1 gives details of the notation and dynamic characteristics of the straddle-type monorail train in service.

The relative displacement can be defined as follows

$$R_{vi1jn} = Z_{v11} - Z_{v2i} + (-1)^n \theta_{vx11}\lambda_{vy2} - (-1)^n \theta_{vx2i}\lambda_{vy2} - (-1)^i \theta_{vy11}\lambda_{vxi} \tag{5}$$

$$R_{vi2jn} = Z_{v2i} - (-1)^j \theta_{vy2i}\lambda_{vx3} + (-1)^n \theta_{vx2i}\lambda_{vy4} - V_{0i2jn} \tag{6}$$

$$R_{vi3jn} = Y_{v2i} - V_{0i3jn} + (-1)^j \theta_{vz2i}\lambda_{vx4} \tag{7}$$

$$R_{vi4jn} = Y_{v2i} - V_{0i4jn} + \theta_{vx2i}\lambda_{vz3} \tag{8}$$

$$R_{vi5jn} = Y_{v11} - Y_{v2i} - \theta_{vx11}\lambda_{vz1} + (-1)^i \theta_{vz11}\lambda_{vxi} \tag{9}$$

where, V_{0imjn} denotes the relative displacement of the bridge and surface roughness at the contact points of wheel positions.

The equation of motion for a traveling monorail train on a bridge can be expressed as indicated below

$$\mathbf{M}_v\ddot{\mathbf{w}}_v + \mathbf{C}_v\dot{\mathbf{w}}_v + \mathbf{K}_v\mathbf{w}_v = \mathbf{f}_v \tag{10}$$

where $\mathbf{M}_v$, $\mathbf{C}_v$ and $\mathbf{K}_v$ respectively represent mass, damping and stiffness matrices of trains. $\mathbf{f}_v$ is the interaction force vector applied on the trains. $\mathbf{w}_v$ indicates the displacement vector of the trains. $(\cdot)$ represents the derivative with respect to time.

2.2 Bridge model

The equation of the forced vibration for a bridge system under a moving monorail train is obtained as shown in Eq. (11), and the Rayleigh damping is adopted to form the damping matrix.

$$\mathbf{M}_b\ddot{\mathbf{w}}_b + \mathbf{C}_b\dot{\mathbf{w}}_b + \mathbf{K}_b\mathbf{w}_b = \mathbf{f}_b \tag{11}$$

where $\mathbf{M}_b$, $\mathbf{C}_b$ and $\mathbf{K}_b$ respectively denote the mass, damping and stiffness matrices of the bridge. $\mathbf{f}_b$ is an external force vector due to the moving monorail train. $\mathbf{w}_b$ indicates the displacement vector of the bridge.

2.3 Monorail train-bridge interaction model

Considering the interaction force/wheel load at the contact points, the combination of Eqs. (10) and (11) gives the equation of the forced vibration for a monorail train-bridge interactive system as follows

$$\begin{bmatrix} \mathbf{M}_b & \mathbf{0} \\ Sym. & \mathbf{M}_v \end{bmatrix} \begin{Bmatrix} \ddot{\mathbf{w}}_b \\ \ddot{\mathbf{w}}_v \end{Bmatrix} + \begin{bmatrix} \mathbf{C}_b & \mathbf{C}_{bv} \\ Sym. & \mathbf{C}_v \end{bmatrix} \begin{Bmatrix} \dot{\mathbf{w}}_b \\ \dot{\mathbf{w}}_v \end{Bmatrix} + \begin{bmatrix} \mathbf{K}_b & \mathbf{K}_{bv} \\ Sym. & \mathbf{K}_v \end{bmatrix} \begin{Bmatrix} \mathbf{w}_b \\ \mathbf{w}_v \end{Bmatrix} = \begin{Bmatrix} \mathbf{f}_b \\ \mathbf{f}_v \end{Bmatrix} \tag{12}$$

where, $\mathbf{C}_{bv}$ and $\mathbf{K}_{bv}$ respectively indicate time-dependant coupling damping and stiffness matrices of the train-bridge interactive system.

2.4 Monorail train-bridge interaction model subjected to ground motion

If the interactive system defined in Eq. (12) is subjected to ground motion, as would be happened in an earthquake, then the problem can be solved by considering an additional force input due to acceleration of the mass that is governed by an absolute coordinate.

The equation of motion for the interactive system under an earthquake in the simplified matrix formation thus becomes as follows

$$\begin{bmatrix} \mathbf{M}_b & \mathbf{0} \\ Sym. & \mathbf{M}_v \end{bmatrix} \begin{Bmatrix} \ddot{\mathbf{w}}_b \\ \ddot{\mathbf{w}}_v \end{Bmatrix} + \begin{bmatrix} \mathbf{C}_b & \mathbf{C}_{bv} \\ Sym. & \mathbf{C}_v \end{bmatrix} \begin{Bmatrix} \dot{\mathbf{w}}_b \\ \dot{\mathbf{w}}_v \end{Bmatrix} + \begin{bmatrix} \mathbf{K}_b & \mathbf{K}_{bv} \\ Sym. & \mathbf{K}_v \end{bmatrix} \begin{Bmatrix} \mathbf{w}_b \\ \mathbf{w}_v \end{Bmatrix} = \begin{Bmatrix} \mathbf{f}_b - \ddot{a}_{base}\mathbf{M}_b \\ \mathbf{f}_v - \ddot{a}_{base}\mathbf{M}_v \end{Bmatrix} \tag{13}$$

where, $\ddot{a}_{base}$ is the ground acceleration at the basement of bridge structures during an earthquake.

Considering projection of equations for the bridge model in the modal space, the derived governing equation of motion for the system is solved by means of Newmark's β method (Newmark 1970) as a numerical integration technique.

3. Comparison of numerical results with field-test data

To verify the validity of the monorail train-bridge interaction model developed here, a monorail bridge with the span length of 34.8 m (see Fig. 4) was tested and analyzed under a moving train. The bridge comprises two steel box track girders, cross beams, bracings, supports and RC piers as shown in Fig. 5. Table 2 shows material properties of the bridge. It is noteworthy that, in bridge modeling, no special calibration was carried out but the existing drawings and design reports are used. On the other hand, for modeling the train, the properties provided by the monorail train manufacturer were used.

The vertical and lateral displacements and acceleration responses of the monorail bridge were measured in field-test. As for the monorail train, vertical and lateral acceleration responses were

Fig. 4 View of the monorail bridge for experiment

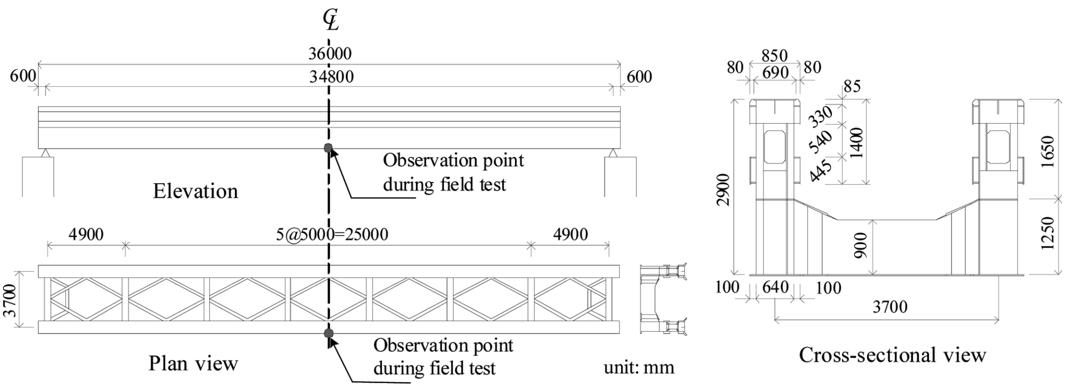

Fig. 5 Configuration of the monorail bridge composed of steel members

Table 2 Material properties of the monorail bridge

Property		Track girder	End cross beam	Cross beam	Lateral bracing
Numbers		2	2	6	28
Young's modulus (GPa)		205	205	205	205
Upper flange	Width (mm)	690	300	300	-
	Thickness (mm)	18	22	19	-
Web plate	Depth (mm)	2782	844	652	176
	Thickness (mm)	14	11	9	8
Lower flange	Width (mm)	840	300	300	200
	Thickness (mm)	19	22	19	10
Yield stress (Mpa)		353	235	235	235

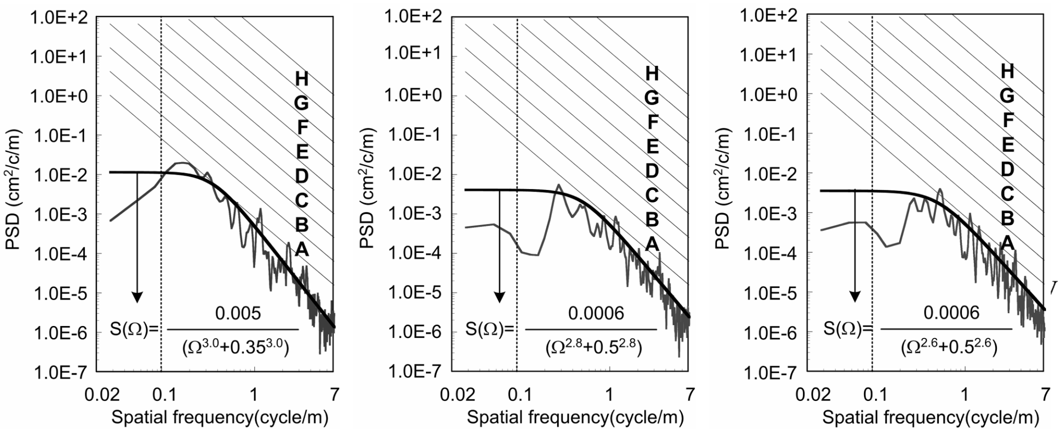

(a) Riding track (b) Steering-guide way (c) Stabilizing-guide way

Fig. 6 Power spectral curves of the measured surface roughness of track-girder

measured. Passenger numbers were also counted during the test. The values described in Table 1 are the properties of the empty monorail train in operation. Field-test involved profiling the surface roughness of tracks for use in dynamic response analysis as well as the seismic response analysis during train moving. Actually, during the profiling the surface roughness, one of wheel paths is measured. Therefore profiles of tracks are generated by means of the Monte-Carlo simulation based on power spectral density curves estimated from the measured profile along one of two paths. It means that, in comparing the analytical result with measured ones, the artificial surface profiles showing the best agreement among 100 samples are used in the analysis. The power spectral density curves taken from the measured profiles were plotted with ISO estimates (ISO 1995) and curve fittings as shown in Fig. 6 to assess the condition of the roughness, in which paved roads are considered to be among roadway roughness classes from A to D, whereas the roadway roughness classes E and F correspond to unpaved roads.

The passenger numbers counted during the test is used in the analysis: 57, 40, 54 and 24 passengers for the first, second, third and fourth passenger cars, respectively. The weight of 588.6 N

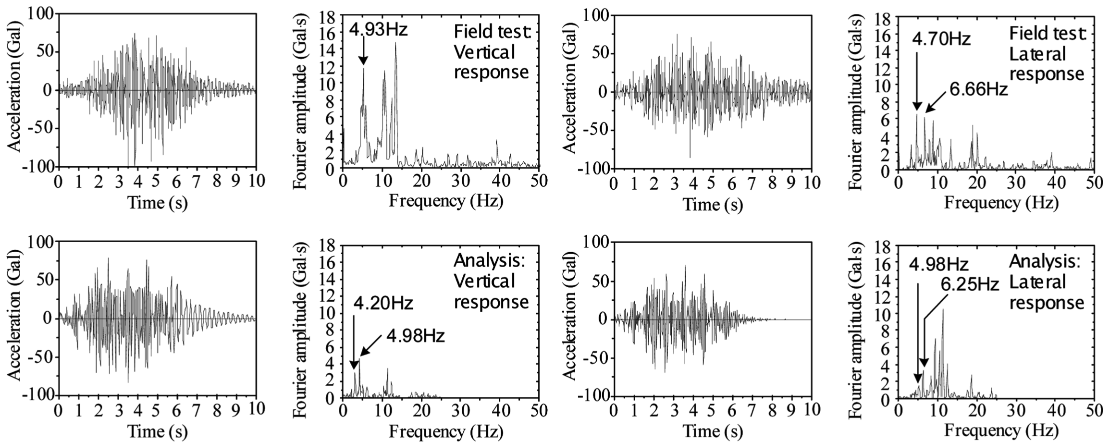

(a) Vertical responses (b) Lateral responses

Fig. 7 Acceleration responses and Fourier spectra of the bridge at the observation point

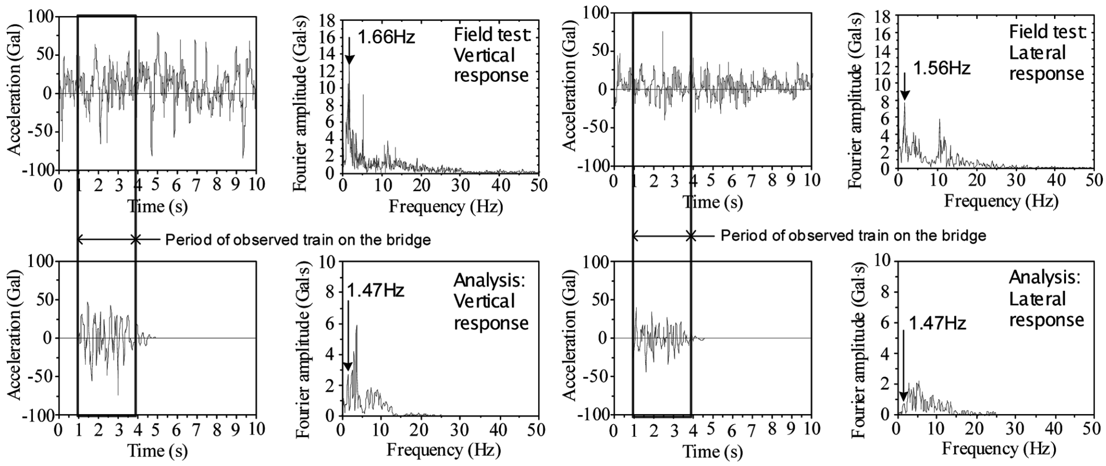

(a) Vertical responses (b) Lateral responses

Fig. 8 Acceleration responses and Fourier amplitude of the monorail train

per person is assumed as the average weight of passengers. The average traveling speed of the train recorded was 55 km/hr, and is used in the analysis.

In dynamic response analysis of the monorail bridge, the response is obtained by superposing up to the 50th modes (f_{50} = 107.9 Hz). The value of 0.25 is used for β of Newmark's β method. The tolerance of 0.001 and one fifth of the highest natural period as the time interval are adopted in the analysis. The damping constant of the monorail bridge is assumed to have 2% for the traffic-induced dynamic response analysis.

The acceleration responses at the observation point of the bridge and the second car in the monorail train, found by analysis and field-testing, are shown in Figs. 7 and 8. Fig. 7 shows that the amplitude of the field-test acceleration in the vertical and lateral directions is slightly greater than that predicted by analysis. The Fourier spectrum shows that the dominant frequencies in field-tests

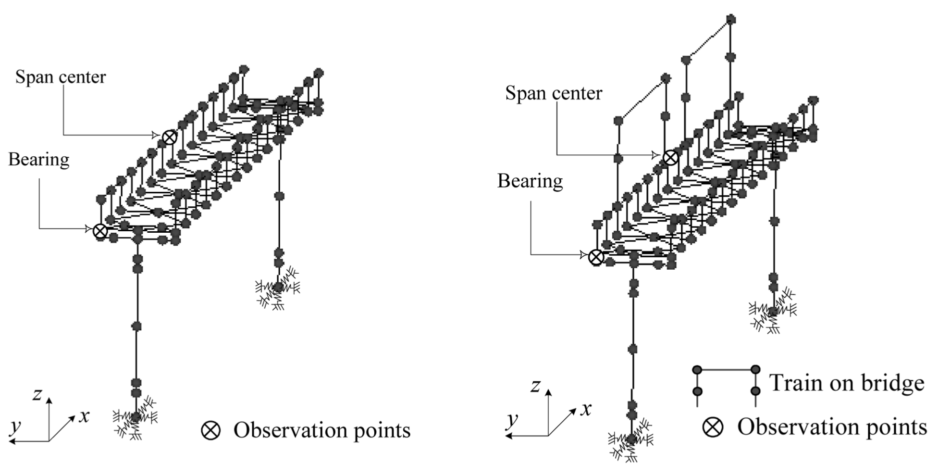

(a) Model considering train as concentrated mass (b) Interaction model of train not moving

Fig. 9 Numerical models

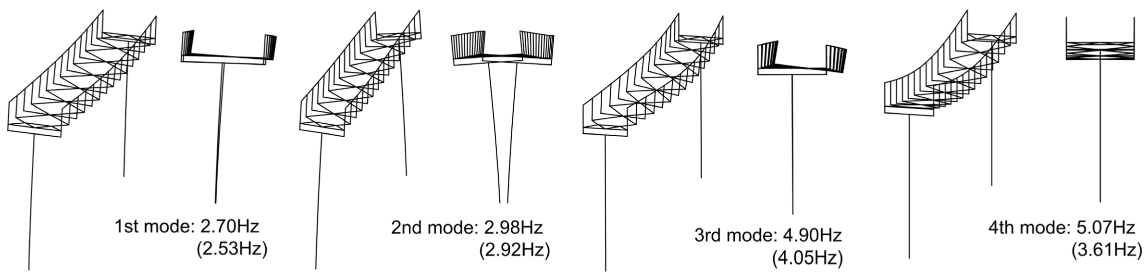

Fig. 10 Natural modes of the numerical bridge model; frequencies in the parenthesis are the natural frequencies of the bridge model considering train as mass

are located near 4.93 Hz and 4.70 Hz respectively for the vertical and lateral responses. Those dominant frequencies of analysis are located between 4.20 Hz and 4.98 Hz for the vertical responses and 4.98 Hz for the lateral responses. Each of the dominant frequency is respectively relative to the vertical and lateral bending modes of 5.07 Hz and 4.90 Hz as shown in Fig. 10.

To examine the dynamic responses of a monorail train, accelerometers for the vertical and lateral directions were installed at a position 1.45 m to the left of, and 2.05 m back from the front axle of the second car in the train. Fig. 8 shows the analytical and experimental acceleration responses of the monorail train. The Fourier spectrum of field-test results shows that dominant frequencies for the vertical and lateral responses are respectively 1.66 Hz and 1.56 Hz. Those dominant frequencies of analytical results are both 1.47 Hz for the vertical and lateral response. The analytical results for acceleration responses of the car in both the lateral and vertical directions also agree well with field test results, even though the hinge between the cars is neglected in modeling the monorail train. As for the spectrum, analytical results on the dominant frequency are observed to have a smaller set of values than those given by field-test. It is noteworthy that the load effect of the passengers counted during field-test is regarded, in analysis, as 60 kg of mass per passenger.

Observations show that measured results have significant additional peaks in the amplitude of acceleration frequency domain compared with the analytic ones. One of the reasons for the phenomenon may be the difference of the train model compared with the real one; that is, the effect of motor, mechanical system, and others of the real train on experimental results may provide the difference. Another reason for the phenomenon may be the difference of surface profiles used in analysis compared with those of experiment even though the most similar surface profile among the simulated profile samples is used in the analysis.

It is a natural consequence to exist differences between experimental and analytical results. Therefore it can be concluded that, in the light of potential sources of error, the trend, wave profile and Fourier spectrum of the theoretical response match well with those of experimental results.

4. Dynamic response subjected to seismic loads

The validity of the seismic response by analysis was verified by comparing with the response taken from the commercial software for the structural analysis (MIDAS GENw). To investigate the effect of train's dynamic system on the dynamic response of the monorail bridge under an earthquake, three numerical examples are examined by means of the three-dimensional method. The first one is the model considering the monorail train as concentrated mass on the bridge model. The second one is the interaction model of the monorail train not moving. The last one is the interaction model with a traveling train. Fig. 9 illustrates the first two numerical models among three models mentioned above because the configuration of the numerical model of a monorail train running is the same as that of Fig. 9(b). The observation points for the acceleration response of the track-girder and shear capacity of the bearing are also shown in Fig. 9.

Representative natural modes and frequencies taken from eigenvalue analysis are shown in Fig. 10. The frequencies in the parenthesis are those of the model considering the train as concentrated mass. The first mode is observed to follow the lateral bending mode of the superstructure coupled with the bending mode of piers. The second mode consists of the torsional mode of the superstructure coupled with the reverse phase of the bending mode of piers. The torsional and bending modes for the superstructure are appeared in the third and forth modes, respectively. In contrast, for the model considering the monorail train as concentrated mass, the bending and torsional modes respectively appear in the third and forth modes.

Fig. 11 exhibits the Level 1 ground motion of moderate soil sites (Group II) (Japan Road Association 2002) considered as the ground motion in the analysis. The damping constant of the

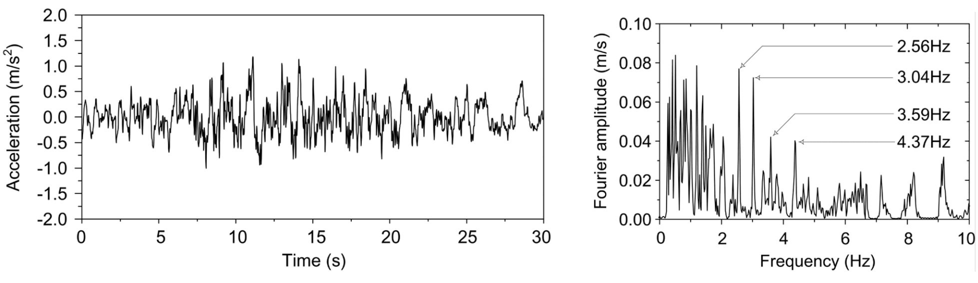

(a) Ground acceleration (b) Fourier spectrum

Fig. 11 Level-1 ground motion of moderate soil sites (Group II) from JSHB

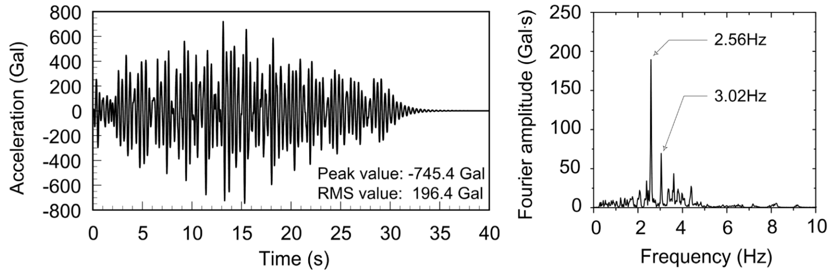

(a) Model considering train as mass

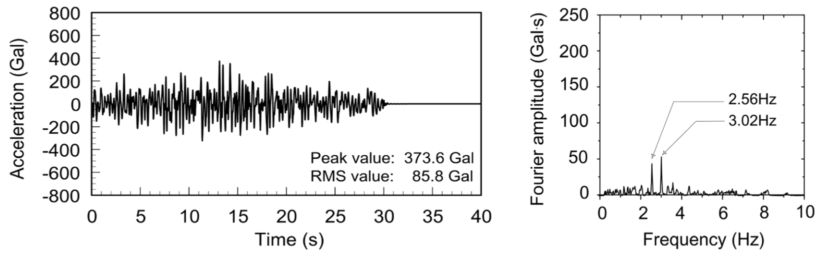

(b) Interaction model of train not moving

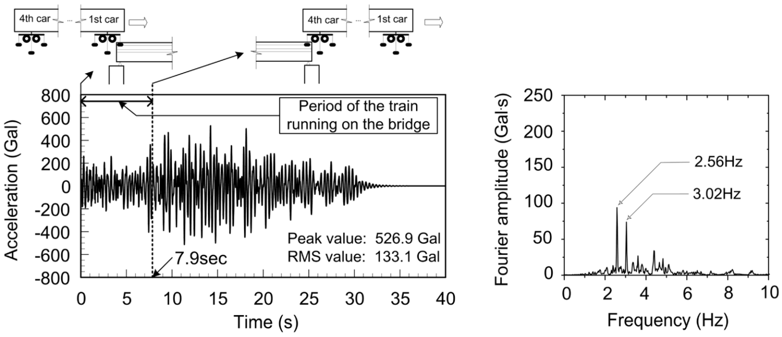

(c) Interaction model of moving train: *v*=11.1m/s

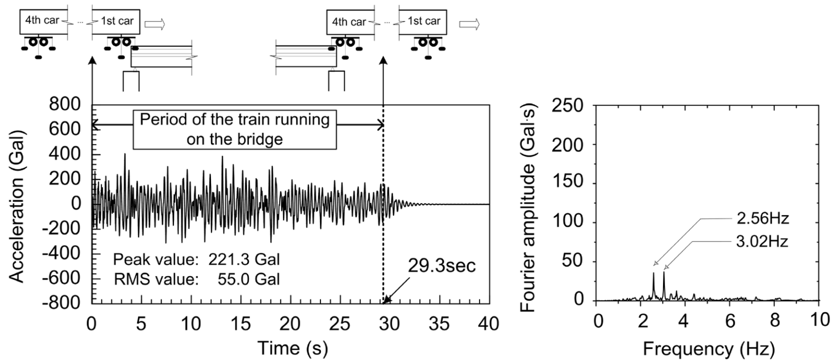

(d) Interaction model of moving train: *v*=3.0m/s

Fig. 12 Transverse accelerations at the span center and Fourier spectra monorail bridge during an earthquake is assumed to have 5% for seismic response analysis.

Acceleration responses at the span center and shear forces at the bearing according to numerical models are summarized in Figs. 12 and 13, respectively. The train speeds of 11.1 m/s (40 km/hr) and 3.0 m/s (10.8 km/hr) are used in seismic response analysis of the bridge to examine the effect of the train speed. The appearance of the dominant frequencies of 2.56 Hz and 3.02 Hz at each Fourier spectrum in Fig. 12 is attributable to the frequency characteristics of the Level 1 ground motion shown in Fig. 11.

It is observed that the models considering train dynamics provide reduction of the peak and RMS values of the acceleration and shear force in comparison with those from the model considering the

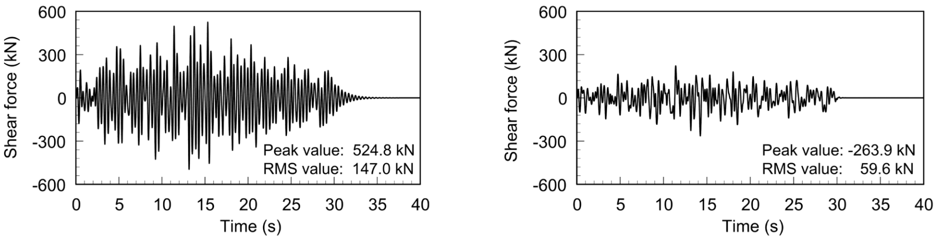

(a) Model considering train as mass (b) Interaction model of train not moving

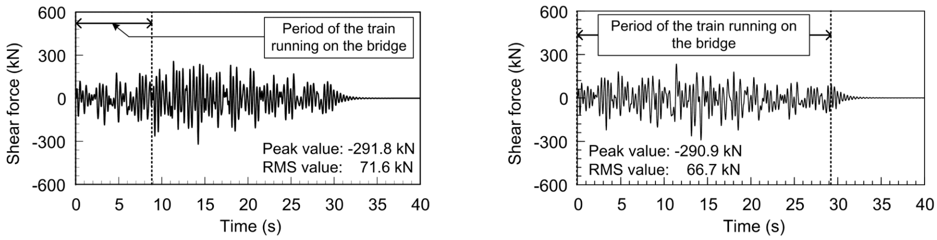

(c) Interaction model of moving train: *v*=11.1m/s (d) Interaction model of moving train: *v*=3.0m/s

Fig. 13 Shearing force at bearing

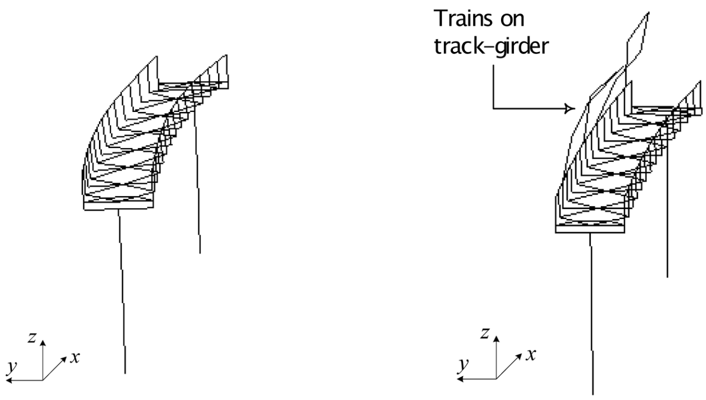

(a) Model considering train as mass (b) Interaction model of train not moving

Fig. 14 Dynamic behavior of monorail trains and bridge under ground motions at $t = 12.0$s train as concentrated mass; decreases of 49.9% and 29.3% in the peak acceleration are obtained due to the models with the train not moving and moving (v = 11.1 m/s), respectively, and, those for RMS values, 56.3% and 32.2% due to the models, respectively; as for shear force, the trends become 49.7% and 44.4% for the peak values, and 59.5% and 51.3% for RMS values according to each model considering train dynamics.

The results obviously demonstrate that the numerical model considering interaction between the bridge and train affects dynamic responses less than the model with train idealized as concentrated mass does. One of the reasons for the phenomenon is that the phase difference depending on the dynamic characteristics of the monorail train and bridge systems helps reducing the inertia effect of the bridge system as shown in Fig. 14, where Fig. 14(b) exhibits the phase difference of displacements between the train and bridge under the Level 1 ground motion. These facts apparently show that the dynamic system of trains acts as a damper under earthquakes.

On the other hand, when the train starts to run the damper effect due to the train's dynamic system on seismic responses of the bridge tends to decrease in comparison with the interaction model of train not moving. One of the reasons is an additional dynamic effect of dynamic wheel loads attributable to the moving train-bridge interaction force because the wheel load during train moving provides an additional dynamic effect on bridge responses. The traveling itself can be another reason because the period that the train can function as a damper is limited according to the

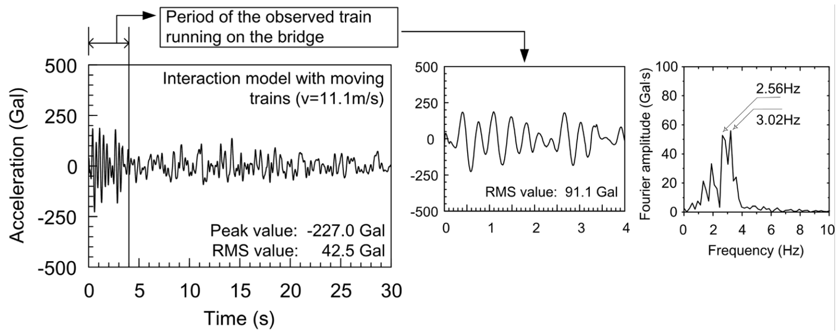

(a) v=11.1m/s

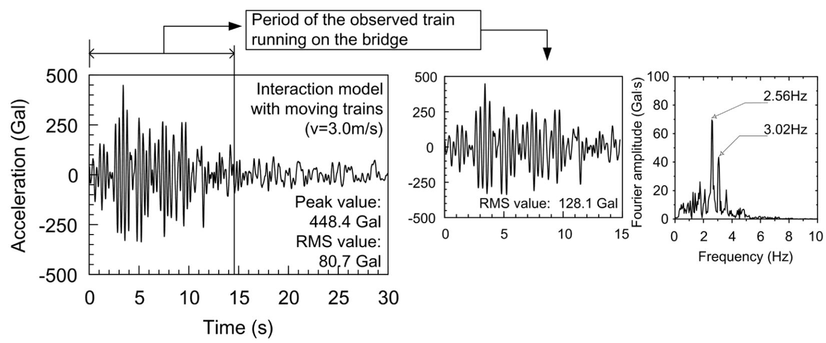

(b) v=3.0m/s

Fig. 15 Accelerations of train body on front axle and Fourier amplitude due to model considering interaction between the moving train and bridge traveling speed of the train; the periods of the train running on the bridge are 7.9 and 29.3 seconds respectively for the speeds of 11.1 m/s and 3.0 m/s. In other words, the acceleration at the span centre and shear force at the bearing due to the train running at $v = 3.0$ m/s (10.8 km/h) (see Figs. 12(d) and 13(d)) have smaller amplitudes than those due to the train with the speed of 11.1 m/s (40.0 km/h) (see Figs. 12(c) and 13(c)).

The acceleration response taken from the train's body of the first car in the running monorail train according to the traveling speed under the Level 1 ground motion is shown in Fig. 15, in which the Fourier amplitude is taken from the acceleration during the car running on the bridge. The dominant frequencies at 2.56 Hz and 3.02 Hz demonstrate that the dynamic response of trains is also strongly governed by the frequency characteristic of the ground motion. The fundamental frequency of train's sway motion was 0.912 Hz for an empty car from the preliminary investigation (Lee *et al.* 2006). For information, those frequencies for bouncing, rolling and pitching were respectively 1.207 Hz, 1.660 Hz and 1.790 Hz. The peak value of the acceleration response within the period of the first car running on the bridge tends to increase with decreasing speed.

5. Conclusions

This study investigates the effect of the dynamic system of monorail trains on seismic responses of a monorail bridge under the Level 1 ground motion of moderated soil site (Group II) earthquake specified in JSHB.

Positive correlations observed between analytical and experimental results verify the validity of developed equations of motion for the monorail train-bridge interaction system.

The seismic response analysis of the monorail bridge provides undisputed evidence that the dynamic system of the train on monorail bridges can act as a damper under earthquakes. This study also suggests that considering the monorail train only as mass in numerical modeling can overestimate the live load effect on monorail bridges. It is worth noting that the damper effect due to the dynamic system of a train on seismic responses of bridges tends to decrease according to the speed of the monorail train. As for dynamic responses of trains, the response increases with decreasing speed.

It needs, however, more investigation to make a specific conclusion, because the dynamic response is affected by many factors such as the span length of bridges, speed, number of passengers, effect of neighboring span, etc. Therefore, the next step for this study will be focused on a parametric study considering the influencing factors.

References

Guyan, R.J. (1965), "Reduction of stiffness and mass matrices", *AIAA J.*, **3**(2), 380.

ISO8608 (1995), *Mechanical Vibration-Road Surface Profiles-Reporting of Measured Data*, ISO.

Japan Road Association (2002), *Japanese Specifications for Highway Bridges, Part V: Seismic Design*.

Kameda, H., Murono, Y., Nanjou, A. and Sasaki, N. (1999), "Earthquake response of highway bridges under bridge-vehicle system", *J. Struct. Mech. Earthq. Eng.*, JSCE, No.626/I-48, pp.93-106 (in Japanese).

Kawatani, M. and Kim, C.W. (2001), "Computer simulation for dynamic wheel loads of heavy vehicles", *Struct. Eng. Mech.*, **12**(4), 409-428.

Lee, C.H., Kawatani, M., Kim, C.W., Nishimura, N. and Kobayashi, Y. (2006), "Dynamic response of a monorail under a moving train", *J. Sound Vib.*, **294**(3), 562-579.

Maruyama, Y. and Yamazaki, F. (2002), "Seismic response analysis on the stability of running vehicles", *Earthq. Eng. Struct. D*, **31**, 1915-1932.

MIDAS GENw, www.midasIT.com.

Miyamoto, T., Ishida, H. and Matsuo, M. (1997), "Running safety of railway vehicle as earthquake occurs", *QR RTRI*, **38**(3), 117-122.

Newmark, N.M. (1970), "A method of computation for structural dynamics", *J. Eng. Mech. Div.,* ASCE, **85**(EM3), 67-94.

Yang, Y.B. and Wu, Y.S. (2002), "Dynamic stability of trains moving over bridges shaken by earthquakes", *J. Sound Vib.*, **258**(1), 65-94.